COBEM 2021 26th International Congress of Mechanical Engineering
November 22-26, 2021, Virtual Congress, Brazil

COB-2021-1989
USE OF METALLIC FUNCTIONALLY GRADED MATERIAL FOR TOTAL HIP ARTHROPLASTY TO REDUCE BONE REABSORPTION DUE TO THE EFFECT OF STRESS SHIELDING

Alexandre Zanni Hubinger
Escola de Engenharia de São Carlos - Universidade de São Paulo, São Carlos-SP
hubinger@usp.br

Jonas de Carvalho
Escola de Engenharia de São Carlos - Universidade de São Paulo, São Carlos-SP
prjonas@sc.usp.br

Fernando Del Monte
Escola de Engenharia de São Carlos – Universidade de São Paulo, São Carlos-SP
delmonte.fernando@usp.br

Yukio Shigaki
Centro Federal de Educação Tecnológica de Minas Gerais, Belo Horizonte-MG
yukio.shigaki@cefetmg.br

Abstract. *Total hip arthroplasty is one of the most successful orthopedic surgeries in modern medicine. The earliest account of hip arthroplasty dates back to 1881. The evolution, since the 1960s, goes through rods with necklaces, textured surfaces for bone growth, stainless steel components under pressure, metal spheres with cemented polyethylene, use of ceramic materials, among others. Osteoarthritis and rheumatoid arthritis are the main causes for performing total hip arthroplasty in elderly and young patients, respectively. Aseptic loosening is the main responsible for revision surgeries and, among several causes, there is evidence that bone loss caused by the effect of stress shielding is one of the main causes. The fact that there is a tendency for patients who undergo total hip arthroplasty to be getting younger and younger, and also that studies show a 20-year survival rate for stems, there is a need to increase that survival. Recently, the evolution of additive manufacturing technologies allows the manufacture of metallic functionally graded materials. In this context, a State of the Art of the main works, recently developed in this area, is presented, focusing on mathematical tools to optimize the material properties of the stems with a metallic functionally graded material according to the mechanical properties of the femur, manufactured by additive manufacture, and on the simulation of the bone resorption process through the finite element method, in comparison to the results obtained with stems manufactured with materials that have homogeneous mechanical properties.*

Keywords: *total hip arthroplasty, additive manufacturing, finite element method, functionally graded material*

1. INTRODUCTION

Total hip arthroplasty (THA) is the term used for surgery that aims to replace the “diseased” hip joint, which is damaged or fractured by a prosthesis with a shape as close as possible to the original anatomy. The oldest report of a hip arthroplasty dates back to 1881 when an ivory ball and joint were attached to the bone with nickel plated screws. Since then, new materials, designs and surgical procedures have been tested by surgeons and researchers. During the 1950s, the use of new design features, textured surfaces for bone growth, stainless steel components, and metal-on-metal articulated components were introduced. These techniques accelerated the rate of development and success producing good clinical results after long follow-up periods. In the mid-1960s, tribological principles and testing methodologies, with the aid of medical skills, led to the development of other types of materials for THA. In modern medicine, THA is one of the most successful surgeries and has been constantly evolving in recent years.

THA is indicated for pathologies such as osteoarthrosis, rheumatoid arthritis, ankylosing spondylitis, Paget's disease, aseptic necrosis of the femoral head and fracture of the femoral neck. According to Ferreira et al. (2017), osteoarthrosis affects 4% of the Brazilian population and is associated with morbidity such as falls, depression and obesity.

Epidemiological and financial studies indicate that the increase in THA has a relevant social and economic impact. A trend was observed in the number of hospitalizations related to THA worldwide, estimating that something around one million of THA are performed each year worldwide. It is believed that this number could duplicate in the next two decades. It has also been noted, in several countries, that THA is being performed on increasingly younger patients. By

2030, it is predicted that 50% of all THA will be performed on patients less than 65 years of age. The accepted lifetime for a hip stem is 15 years, with some studies finding a survival of up to 22.6 years.

In general, aseptic loosening is one of the most responsible for prosthesis revision. There are indications that bone loss caused by the effect of stress shielding is one of the main ones. This phenomenon occurs due to the difference between the modulus of elasticity of the femur bone and the material used to manufacture the implanted stem. When the femur bone is partially replaced by a more rigid metal stem, there is a redistribution of mechanical stimuli in the bone, resulting in a decrease in stresses in the proximal region of the femur and, as the bone is a living tissue that reacts to mechanical stimuli, it can be partially reabsorbed.

In recent years, studies have been carried out with the objective of obtaining a non-uniform distribution of the mechanical properties of the stem material, for example, the modulus of elasticity, using what we call functionally graded materials (FGM). The ideal mechanical properties for reducing bone resorption, due to the stress shielding effect, of FGMs are determined by optimization algorithms that use finite element analysis (FEA) softwares to determine the acting stresses and even simulate bone remodeling. Due to advances in additive manufacturing techniques, the FGMs can be manufactured by varying the porosity of the material that constitutes the stem used for THA

2. ADDITIVE MANUFACTURING

Recent progress in Additive Manufacturing (AM) technologies has allowed for the development of novel applications in various industries. Some of these applications include the planning of surgical operations, printing of biodegradable tissues, and, most importantly, the development of orthopedic implants. The application of reverse engineering in AM technology ensures the customization of the printed implants. This process starts with data acquisition or obtaining the exact anatomical data from scanning techniques, such as computed tomography (CT) or magnetic resonance imaging (MRI). The two dimensional images can be converted in three dimensional computer aided design model (CAD) using specialized software and the model can be converted to be used in a FEA.

Different materials have been developed to suit the numerous functions of the orthopedic implants. For instance, most of the loads bearing implants are fabricated from metallic materials like titanium alloys and cobalt-chromium alloys. One downside of metallic materials is the high stiffness and weight but a lot of research has been directed to reduce their stiffness and weight. The most significant benefit of reducing the stiffness of the metallic material used in orthopedic implants is to avoid the stress shielding phenomenon that is associated with the fact the stiff metal implanted beside the bone will bear most of the load, leaving the bones with less load. Conforming to Wolff's Law, bone requires continuous mechanical stimulation to regrow, or else it will start reducing its mass by getting thinner or becoming more porous.

The use of porous metallic materials has been considered in AM for reducing metallic material stiffness and also, from the biological point of view, has better osseointegration. Another advantage of AM is the possible printing of FGM that vary in composition or microstructure following a certain design law.

The powder bed fusion (PBF) is one of the most common AM technologies used to print metallic orthopedic implants. An energy source, like electron or laser beam, is used to selectively melt parts of the powder bed based on the data fed to the machine. When one layer is fused, the building platform is lowered by a predetermined distance via a piston. A mechanical coater, blade or roller, places a new layer of powder on top of the platform, and the process is repeated until the final shape has been reached. The two main PBF technologies that can print metallic parts are Electron Beam Melting (EBM) and Selective Laser Melting (SLM).

SLM and EBM are both more accurate and can achieve a better resolution and can be used to print lattice structures. The high energy resulted from the EBM is attributed to the electron energy source, thus fully dense parts can be printed. SLM has higher cooling rate than EBM, resulting in coarser microstructure, higher tensile strength, and lower ductility than parts. SLM was used to produce commercial pure titanium samples with mechanical properties than conventional methods and its cooling is also higher, which resulted in finer microstructure and therefore produced more desirable mechanical properties.

3. FUNCTIONALLY GRADED MATERIALS

FGM can be classified into three distinct groups: gradient microstructure, gradient composition, and gradient porosity as we can see in a schematic illustration in figure 1. A material with varying microstructure along its volume could be achieved by controlling heat treatment. The advantage of this technique is that a tougher core can be obtained, with a hardened surface that would increase wear resistance. Although this technique has not been applied in the biomedical realm, it suggests a direction for improving the hardness of articulating surfaces.

The functionally graded composition can be defined as "A change in composition across the bulk volume of a material aimed to dynamically mix and vary the ratios of materials within a three dimensional volume to produce a seamless integration of monolithic functional structures with varied properties" (Pei et al., 2017). It is used to provide a enhanced substitute for the coating in orthopedic implants.

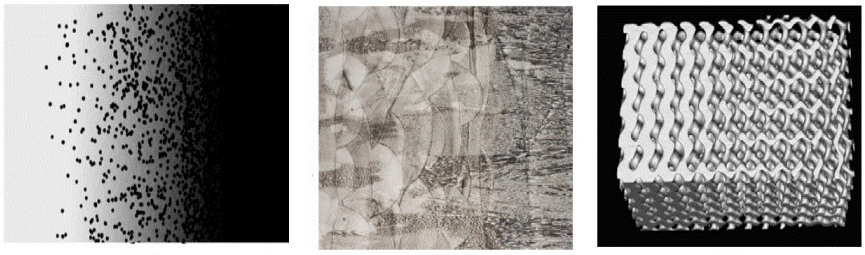

Figure 1: Classification of FGM according to (a) composition; (b) microstructure; (c) porosity (Mahmoud and Elbestawi, 2017)

Functionally graded porosity can be created in materials by changing the porosity across the bulk volume. The variation in density will combine variation in mechanical properties, which can make the part more functional than a single constitutive material for some applications. Parts of the implants with low porosity have high mechanical stability, while high porosity regions support bone ingrowth and help with the implant's fixation. AM techniques remains an attractive method for fabricating functionally graded porosity, using lattice structures, with the required geometry and precise control of unit cells.

The term lattice structure is often used in the literature but, in fact, the lattice structure is one type of cellular material. Cellular materials are usually classified according to their porosity type and their building unit cells order. There are several applications for cellular materials; one of them is the biomedical implants. Lattice structures are characterized by open pores and non-stochastic orientations of the building unit cells. This unit cell geometry and topology are used to tailor the mechanical properties of the part. A CAD based unit cells is showed in figure 2.

Figure 2: CAD based unit cells designs of lattice structures used in biomedical implants (Mahmoud and Elbestawi, 2017)

4. FEMUR STEMS USING FUNCTION GRADED MATERIALS TO REDUCE BONE REABSORPTION

The first fully porous femoral stem with tunable properties that minimize bone reabsorption as a result of stress shielding was developed by Arabnejad et al. (2016). To develop the porous hip implant, a finite element model of the femoral bone was created by processing CT scan data of a 38-year-old patient bone. To achieve this goal, were used radiographic density of CT images, quantified as Hounsfield Unit (HU), to represent the local material properties of the human femur. The apparent density for each finite element of the femur model is then determined from the Hounsfield value measured from computed tomography data. From the apparent density distribution, the effective elastic moduli of the bone were obtained using a relation. Bone is treated as an isotropic material.

The macro geometry of the hip implant has a tapered edge shape. Mechanical properties, in particular the homogenized stiffness tensor and the multi axial yield surface, are calculated via Asymptotic Homogenization theory.

To obtain the optimum relative density distribution throughout the implant to minimize bone reabsorption secondary to stress shielding, it was discretized the three dimensional implant with 75 sampling points on the medial-lateral plane of the implant, as showed in figure 3(a). The interior micro-architecture of the implant, figure 3(b), was obtained for a femur loaded under the physiological loading and boundary conditions. The forces, acting forces points, and boundary conditions applied correspond to the gait cycle.

Material architecture tailoring is achieved by minimizing bone resorption subjected to a set of inequality constraints, including the fatigue safety factor and the interface failure. The study used the Tsai-Wu failure criterion for the failure analysis of the lattice under multi axial and fatigue conditions.

The amount of bone loss around the stem is determined by assessing the amount of bone that is under loaded post implantation relative to the intact femur. Bone can be considered locally under loaded when its local strain energy per unit of bone mass is beneath the local reference value which is the value when no prosthesis is present.

The architected fully porous implant was manufactured with (SLM) technique, figure 3(c).

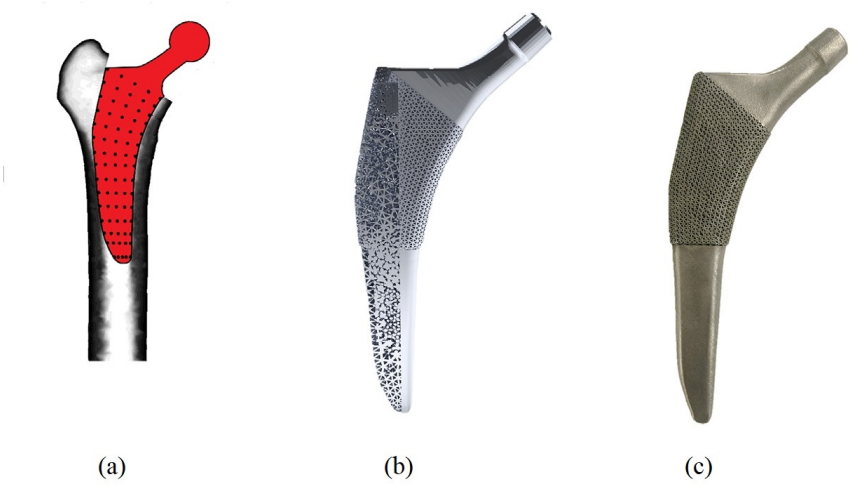

Figure 3: (a) Three dimensional implant to be optimized, (b) Implant micro architecture, (c) Implant fabricated via SLM (Arabnejad et al., 2016)

The resultant amount of bone resorption for the optimized implant is presented in figure 4 and compared with the amount of bone resorption secondary to stress shielding for the fully solid implant. The physiological finite element analysis model shows a total of 34% of bone resorption secondary to stress shielding for the fully solid implant, and 8% in the optimized fully porous implant. This indicates a greater than 75% reduction in bone loss secondary to stress shielding. The fully porous implant can realize 8% volumetric bone loss in Gruen zone 7, whereas the fully solid implant 27% in zone 7, followed by 5% in Gruen zone 6, and 2% bone loss in Gruen zone 2.

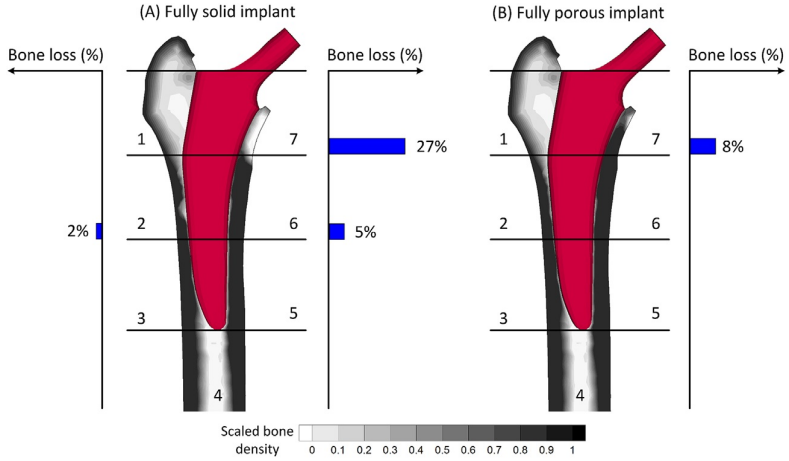

Figure 4:Volume bone loss for the Gruen zones of the femur (Arabnejad et al., 2016)

Limmahakhun et al. (2017), used a CT of a 60 year old woman to extract three dimensional models using the Amira (FEI, USA) software. The values between 148 and 1872 Hounsfield Units were used to the tissue threshold of a femoral bone. They used the CAD SolidWorks (USA) software to design a femoral stem with 120cm length. This stem received a modified tapered stem adapted from a commercial implant to match the internal geometry of the femur canal. Based on the axial and radial planes, the proximal part of femoral stem was sliced.

The parameters of femoral head heights, head offset distance, and femoral neck anteversions between a femoral bone, before and after the implantation, with no difference was controlled during the proceeding to perform the visual operation in computer aided design software to replace the femoral stem.

The different types of bone of the femur were considered as a homogeneous, isotropic and linear elastic material. The elastic modulus in the cortical bone was considered 17GPa and in the cancellous bone 0.4GPa. A laser melted CoCr cellular structure with porosity between 14% - 67% was assigned to each part based on graded patterns, the elastic modulus for the used porosity are showed in table 1.

Four types of CoCr graded femoral stems were studied and compared with the Ti femoral stem. Figure 5 shows the four types of stems used in the study: a radially graded stem with a stiffer inner core (dense RGS), another radially

graded stem with a stiffer outer cortex (hollow RGS), an axially grades stem with a stiffer proximal end (proximal AGS), and an axially graded stem with a stiffer distal (distal AGS).

Table 1: Material properties of CoCr cellular structure (Limmahakhun et al., 2017)

Materials	Elastic modulus (GPa)	Yield strength (MPa)	Max strength (MPa)	Strength to modulus ratio
CoCr porosity 67%	2.33	36	113	48.5
CoCr porosity 54%	2.65	67	284	107
CoCr porosity 44%	2.98	110	453	152
CoCr porosity 41%	3.14	130	523	167
CoCr porosity 14%	5.26	299	916	174
CoCr	200	600	1100	5.5
Ti	116	795	860	7.5

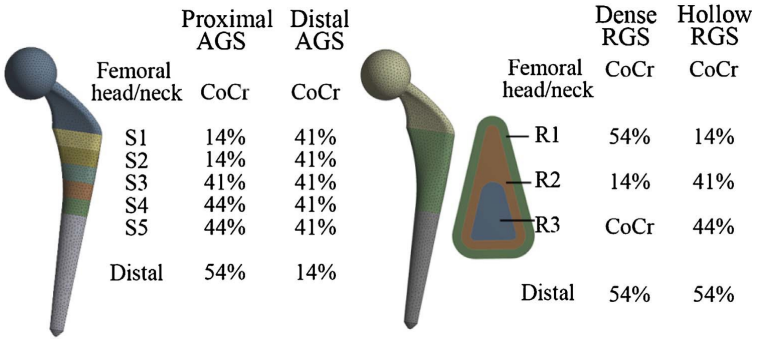

Figure 5: The geometry and material assignments of CoCr graded femoral stems (Limmahakun et al., 2017)

The finite element software ANSYS 16.1 (Ansys, Inc.) was used to model bone and graded femoral stem configurations following a continuous approach. Both primary and secondary stage stem stability were modeled. In the primary stage, non-osseointegration, a large sliding surface-to-surface contact elements with purely frictional behavior was applied to simulate the bone-implant interface

Only main muscle, abductor muscle, which attaches to the greater trochanter and the hip joint reaction were considered in the loads applied on the circular surface. The forces used were derived from a person walking in a single-leg stance phase. During the gait cycle, the greatest loading forces around a prosthesis occur during the stance phases. To prevent body motion, the distal end of the femur was fully constrained.

Parametric study with material properties based on the graded patterns were optimized by which could match the objective of relative micromotions < 150μm. This relative micromotion occurs along the constructive paths of medial and lateral bone-implant interfaces. The optimized material combinations which maintained micromotions in the adequate range, resulted from the parametric study, are showed in figure 5. The proximal AGS, dense RGS, and hollow RGS models successfully control the amount of bone-implant interfacial micromotions. The distal AGS shows an increase risk of implant stability from the clinical point of view.

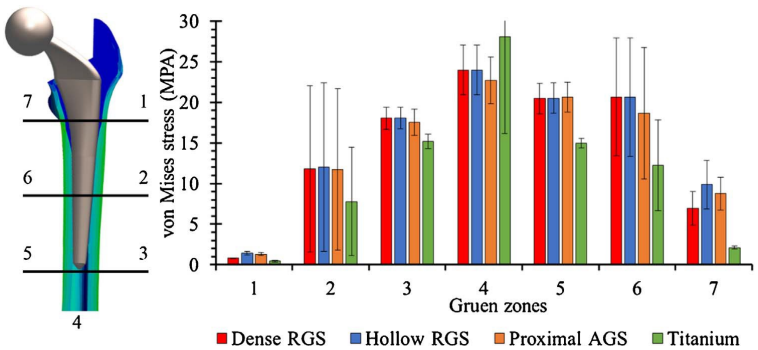

Figure 6: Comparison of the average von Mises stress values between femoral stems in the seven Gruen zones. (Limmahakhun et al., 2017)

In the secondary stage, osseointegrated, both implants and femurs were considered assumed completely bonded along the bone implant interfaces. The press-fit effect was not considered. For all the implants and femurs, the Von Mises stresses and principal stresses were analyzed to investigate any risk of failure under loadings. The von Mises

stress along the bone-implant interfaces was used as an indicator of the stress-shielding effect, figure 6. The stress values were divided into seven Gruen zones to compare their mean values between the four designs of CoCr graded femoral stems. Despite the design, the extent of stress shielding is directly related to the stem's stiffness. Ti femoral stem shows the minimum and maximum stress values found in Gruen zones 1 and 4 respectively.

Using AM, SLM process, the optimum designs of graded femoral stems obtained from finite element analysis and the CoCr solid femoral stem, control model, were selected to fabricate. The building direction was aligned along the longitudinal axis of the stem.

A three dimensional model of a normal femur was constructed by Sun et al. (2018) from computed tomography images using Mimics 16.01 (Materialise, Belgium) and Geomatic 12 (Geomatic, USA) software. In sequence, the model was resected in the distal region and them, meshed in ABAQUS 6.14 (Dassault, France). A relation between the gray scale value of the CT data, Hounsfield Unit (HU), and the density of the bone was used to map the material properties, elastic modulus, of individual elements. In figure 7, is presented the distribution of the elastic modulus of the femur.

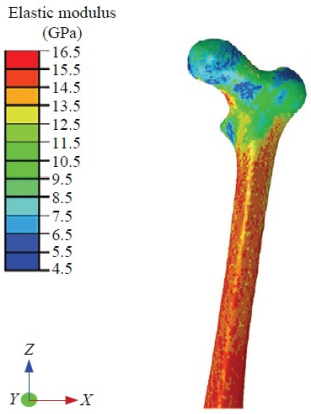

Figure 7: The modulus distribution in the femur (Sun et al., 2018)

A typical cementless femoral stem was employed in this study. Its implantation was carried out according to the clinical requirement under the guidance of an orthopedist. Using ABAQUS 6.14 software, the finite element model of the bone-implant assembly was built and, using penalty contact algorithm as small sliding surface-to-surface contact, the interface between medullary cavity and the stem was defined. The femur was fixed at distal section and, at the virtual center of the femoral head, joint force was applied. According to the hip anatomy, the orientations and magnitude of the muscle forces were applied on the femur. Linear tetrahedron elements were used to mesh both the femur and the stem.

In the design procedure, considering the manufacturing feasibility of porous structure by SLM of Ti_6Al_4V as well as the elastic modulus of cortical bone, modulus of implant elements varied in a range of 15GPa and 110GPa. Then, the middle part of femoral stem was set as region of interest and the initial modulus of this region was set as 15GPa, and the necking and distal end were set as 110GPa, which remains constant in subsequent iterative calculations. The purpose of subsequent iterative calculations was to achieve the structural safety.

After the initialization, the global safety factor was calculated by the finite element analysis of the bone-implant model. If it is less than the goal value for the safety factor means that not all the part of the prosthesis meets the strength requirements and the elastic modulus of elements need to be reassigned. In the algorithm developed, the elements with high value of Von Mises stress would be assigned with low modulus and vice versa.

The interior region close to the axis of stem bearing low stresses was assigned with high modulus, and the exterior region was assigned with low modulus. Therefore, the elastic modulus of the stem changed in gradient from inside out, in similar pattern to that of stress distribution in the stem. Finally, elements with modulus higher 100GPa were defined as solid element and were removed from the region of interest in the next iteration.

The finite element model with adaptive elastic modulus was calculated until the global safety factor was reached. The value for the safety factor was set to be 10 for safety precaution, considering the difference between the fatigue strength and static compressive strength of porous structure. The procedure described was run in ABAQUS software under the control of the Python language script.

The Huiske's bone adaptation law was used to evaluate the bone remodeling in accordance to the change of bone density. The strains of the bone implanted with three models of hip stem: solid model with elastic modulus of 110GPa (stem-H), high-porosity model with low elastic modulus of 15GPa (stem-L), and the designed model with gradient modulus distribution (stem-D), as showed in table 2, were determined by finite element analysis. A post-processing script written in Python from the output results database were used extract the data of bone strain.

Table 2: Definition of contrast models (Sun et al., 2018)

Model name	Elastic modulus distribution	
	Neck and distal end	Region of interest
Stem-H	110GPa	110GPa
Stem-L	110GPa	15GPa
Stem-D	110GPa	Optimized

After seven iterations, the optimized design of the hip stem was obtained. The mean elastic modulus for the region of interest was 89GPa, and the corresponding porosity was 11%. The elastic modulus gradually reduced from the central axis of the stem towards outside radially, and the proportion of high modulus decreased gradually towards distal stem. The global safety factor was 11.3 for the designed stem-L and 26,4% elements were designed as solid and funnel-shaped distribution was extended along the axis of the stem, figure 8. For the stem-L the safety factor was 4,5.

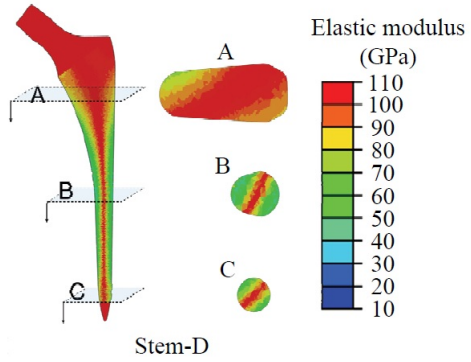

Figure 8: The elastic modulus distribution of stem-D (Sun et al., 2018)

In agreement with the clinical practice and computational results from the literatures, the density loss occurred near the proximal medial femur in all cases. The total volume of the bone with density loss in the case of the stem designed, stem-D, was 9,2%, which was nearly 40% lower than that of the solid model with elastic modulus of 110GPa, stem-H, but still higher than the high-porosity model with elastic modulus of 15GPa, stem-L.

In the study of He et al. (2018), they applied a finite element method to investigate the effect of the stress shielding and to optimize an implant design. Three models were constructed, the first model, figure 9(a), was an intact femur model where computed tomography scan (CT) and three dimensional CAD model of femur were used to capture the geometry and to distinguish cortical bone and cancellous bone. It consists of a layer of cortical bone on the outer surface, and cancellous bone in the inner space. The software Altair HyperWorks 14 was used to build and solve the model. The others two models were a femur with a generic implant and a femur with an optimized implant, figure 9(b).

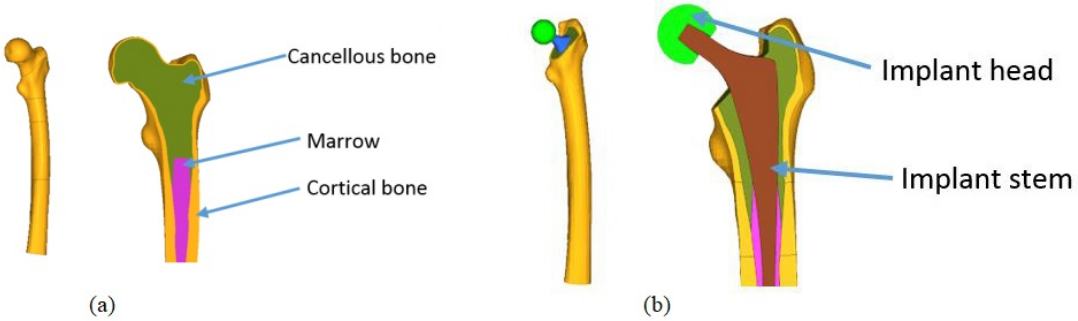

Figure 9: (a) Femur bone model and cross-section view; (b) Femur with generic implant and cross-section view (He et al., 2018)

The representation of a structural configuration after a total hip arthroplasty was obtained sectioning near the greater trochanter of the femur and positioning the implant into it. The procedure, mimic a standard femoral neck resection. To fix the implant stem and femur bone was used freeze contact that has little effect on the bone stresses and, also, simplify the problem to reduce the optimization time of the implant.

Although the mechanical properties of the femur bone are however not homogeneous or isotropic, all the material in the finite element method were considered as isotropic materials except for the cortical bone, which was modeled as an orthotropic material, figure 10(a). In table 3, are listed the sections of the finite element model and their respective material properties. The stiffer direction E1 of the orthotropic cortical bone, were aligned with the load path, figure 10(b).

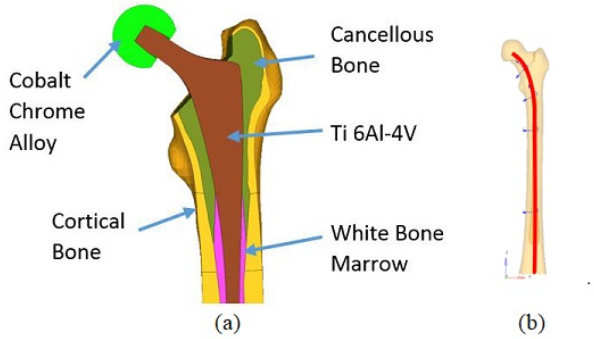

Figure 10: (a) Material assignment in FE model; (b) Red line shows cortical bone E1 direction (He et al., 2018)

Table 3: Material properties (He et al., 2018)

Sections	Material	Elasticity Modulus (GPa)	Poisson's ratio	Density (g/cm^3)
Implant head	Cobalt-Chrome alloy	220	0.30	8.29
Implant stem	Ti-6Al-4V	114	0.30	4.51
Spongy bone	Cancellous bone	1,0	0.30	0.45
Marrow	White bone marrow	0,30	0.45	1.00
Outer femur layer	Cortical bone	E1 = 17.0 G12 = 3.30 E2 = 11.5 G23 = 3.60 E3 = 11.5 G31 = 3.30	ν_{12} = 0.58 ν_{23} = 0.31 ν_{31} = 0.31	1.80

Seven loads cases were used in the study. These loads cases characterized femur loads for standing-up, standing, going up stairs, and jogging. Also were used a combined load case, and two ISO Standard load case (ISO7206-4 and ISO7206-6). The ISO load cases were included to ensure the design has a good fatigue strength.

Changes in strain energy or stress were measured to evaluate the stress shielding effect. The strain energy had equivalent meaning as "Compliance" in the solver and optimizer procedure and it was used to measure the stress shielding effect. They used the "Stress Shielding Increase" (SSI) using the stresses before and after the THA for each element in the femur. A smaller SSI value means less stress shielding. The stresses used for calculate de SSI value correspond to the Von Mises stresses because it is a non-negative value that indicates the stress level.

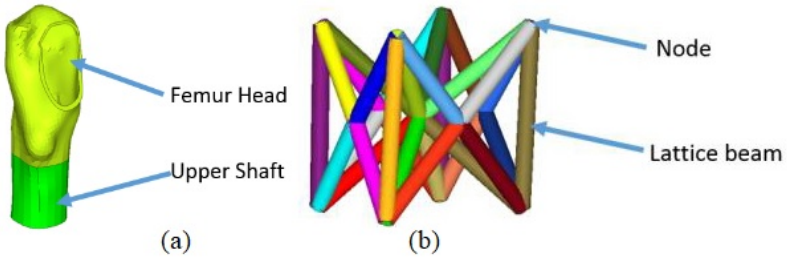

Figure 11: (a) Femur head and upper shaft, (b) Face and body centered cubic with vertical structs unit cell (He et al., 2018)

The generic implant stem was utilized as the design space excepting the neck region. The upper portion of the femur cortical bone was divided into "Femur Head" and "Upper Shaft" sections, figure 11(a). A regional compliance was used to control the stress distribution better as the research showed that the cortical bone of the upper femur is subjected to a more severe effect of stress shielding, so the deformation energy of this region was investigated. Some manufacturing constraints, like draw and extrusion, were applied to help understand and interpret the topology results. Minimizing global compliance was the objective function to obtain the most efficient structure.

From the topology optimization results, the solid material zones were represented with shell and tetra elements. Semi-dense regions of the topology use a face and body-centered cubic with vertical struts unit cells, figure 11(b). The design must be printed in the vertical position which ensures manufacturability. The unit cell size is 4-7mm, varying across the implant. The lattice was constructed with 1D beam elements since their diameters can be easily parameterized with the optimization procedure. The diameters of the lattice beams were the design variables. Beam diameter can vary from 0.5mm to 2.0mm based on the manufacturability and cell size. The part that corresponds to the skin shell thickness can vary between 0.5mm to 5.0mm. In the ISO standard load cases, the Von Mises stress of the implant should be no greater than 600MPa to have a safe margin. To save material and printing time was set, as the optimization objective, to minimize the total volume.

After the optimization procedure, a solid-lattice design of the implant was proposed where the bottom tip was made solid with a smooth surface, figure 12(a). The optimized implant leads to an average of 57,3% lower SSI value over the five load cases than the generic implant, and it was validated against ISO7206-4 and ISO7206-6 load cases, where the maximum stress is 575MPa indicating the optimized implant meets the fatigue standard. The prototype of the optimized implant was printed, using the material Ti_6Al_4V alloy, with a SLM machine, figure 12(b).

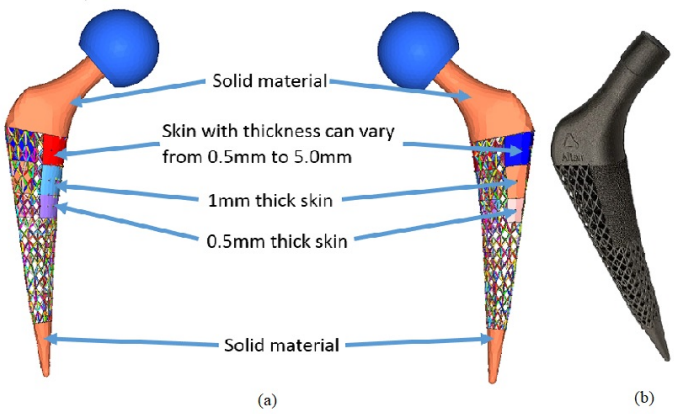

Figure 12: (a) Solid lattice implant design space, (b) EOS printed Titanium solid-lattice hip implant (He et al., 2018)

5. CONCLUSIONS

In the studies, many design methodologies were presented to determine the elastic modulus distribution in the stems used in THA for better match between the implant with that the residue bone tissue in terms of the stiffness. The elastic modulus distribution is result of use of high strength functionally graded materials with different internal microstructure that contributes to vary the material porosity compared with fully materials. The results showed that the use of FGM, manufactured by AM techniques, in stems for hip implants, could contribute to reduce the bone reabsorption secondary to stress shielding effect. Actually, the methodology can be used to design standards hip stems but, in the future, customized prostheses can be designed and manufactured with each patienty's femur geometry and bone material properties that are captured by computed tomography, achieving the optimal hip stem for each individual.

6. REFERENCES

Arabnejad S., Johnston B., Tanzer M., and Pasini D., 2016. "Fully porous 3D printed titanium femoral stem to reduce stress-shielding following total hip arthroplasty", *Journal of Orthopaedic Research*, August 2017, p. 1774-1783.

Gong H., Wu W., Fang J., Dong X., Zhao M., and Guo T., 2012. "Effects of materials of cementless femoral stem on the functional adaptation of bone", *Journal of Bionic Engineering*, Vol. 9, p. 66-74.

Gong H., Kong L., Zhang R., Fang J., and Zhao M., 2013. "A femur-implant model for the prediction of bone remodeling behavior induced by cementless stem", *Journal of Bionic Engineering*, Vol. 10, p. 350-358.

He Y., Burkhalter D., Durocher D., and Gilbert J.M., 2018. "Solid-lattice hip prosthesis design: applying topology and lattice optimization to reduce stress shielding from hip implants", In *Proceedings of the 2018 Design of Medical Devices Conference*, April 9-12, Mineapolis, USA.

Khanok S.A. and Pasini D., 2012. "Multiscale design and multiobjective optimization of orthopedic hip implants with functionally graded cellular material", *Journal of Biomechanical Engineering*, Vol. 134, p. 031004.

Limmahakhun, S., Oloyed A., Chantarapanich N.,Jiamwatthanachai P., Sitthiseripratip K., Xiao Y., and Yan C, 2017. "Alternative designs of load – sharing cobast chromium graded femoral stems", *Materials Today Communications*, Vol. 12, p. 1-10.

Mahmoud, D. and Elbestawi, M.A., 2017. "Lattice structures and functionally graded materials applications in additive manufacturing of orthopedic implants: a review", *Journal of Manufacutring and Materials Processing*, 12 October 2017.

Oshkour A.A., Abu Osman N.A., Bayat M., Afshar R., and Berto F., 2014. "Three-dimensional finite element analyses of functionally graded femoral prostheses with different geometrical configurations", *Materials and Design*, Vol. 56, p. 998-1008.

Pei E., Loh G.H., Harrison d., de Amorim Almeida H., Monzón Verona M.D., and Paz R., 2017. "Exploring the concept of functionally graded additive manufacturing", *Assem. Autom.*, Vol. 37, p. 147-153.

Sun C., Wang L., Kang J., Li D., and Jin Z., 2018. "Biomechanical optimization of elastic modulus distribution in porous femoral stem for artificial hip joints", *Journal of Bionic Engineering*, Vol. 15, p. 693-705.

Yamako G., Janssen D., Hanada S., Anijs T., Ochiai K., Totoribe K., Chosa E., and Verdonschot N., 2017. "Improving stress shielding following total hip arthroplasty by using a femoral stem made of β type Ti-33.6-4Sn with a Young's modulus gradation", *Journal of Biomechanics*, Vol. 63, p. 135-143.

7. RESPONSIBILITY NOTICE

The authors are the only responsible for the printed material included in this paper.